Biochimie (1991) 73, 879–886
© Société française de biochimie et biologie moléculaire / Elsevier, Paris

The interplay between X-ray crystallography, neutron diffraction, image reconstruction, organo-metallic chemistry and biochemistry in structural studies of ribosomes

M Eisenstein[1], R Sharon[1], Z Berkovitch-Yellin[1,2], HS Gewitz[3], S Weinstein[1,3]
E Pebay-Peyroula[4], M Roth[5], A Yonath[1,2]*

[1]*Department of Structural Chemistry, Weizmann Institute, Rehovot, Israel;*
[2]*Max-Planck-Research Unit, Hamburg;*
[3]*Max-Planck-Institute for Molecular Genetics, Berlin, Germany;*
[4]*J Fourier University and Institute Laue-Langevin, Grenoble;*
[5]*LIP–CEA, Grenoble, France*

(Received 12 November 1990; accepted 13 March 1991)

Summary — Crystals of ribosomes, their complexes with components of protein biosynthesis, their natural, mutated and modified subunits, have been subjected to X-ray and neutron crystallographic analyses. Electron miscroscopy and 3-dimensional image reconstruction, supported by biochemistry, genetic, functional and organo-metallic studies were employed for facilitating phasing of the crystallographic data. For example, a monofunctional multi heavy-atom cluster (undecagold) was designed for covalent and quantitative binding to ribosomes. The modified particles were crystallized isomorphously with the native ones. Their difference-Patterson maps contain indications for the usefulness of these derivatives for subsequent phasing. Models of the ribosome and its large subunit were reconstructed from tilt series of 2-dimensional sheets. The comparison of the various reconstructed images enabled an initial assessment of the reliability of these models and led to tentative assignments of several functional features. These include the presumed sites for binding mRNA and for codon–anticodon interactions, the path taken by the nascent protein chain and the mode for tRNA binding to ribosomes. These assignments assisted in the design of biologically meaningful crystal systems. The reconstructed models are being used to identify structural features in initial density maps derived from X-ray and neutron diffraction data.

ribosomes / crystallography / neutron diffraction / 3-dimensional image-reconstruction / derivatization

Introduction

Ribosomes are notoriously unstable and flexible, hence very difficult to crystallize. Nevertheless, we have obtained 17 different crystal forms of various ribosomal particles and are collecting crystallographic data from 6 of them [1–7]. All crystal types obtained in our laboratory are of biologically active ribosomes.

Two of these, namely the large ribosomal subunit (50S) from *Halobacterium marismortui* and the small one (30S) from *Thermus thermophilus* diffract X-rays almost to molecular resolution: 4.5 and 7.3 Å respectively [3, 4].

Two rather similar forms of the whole (70S) ribosome from *T thermophilus* [8], and of its complex which mimics a defined functional state [6], diffract well to low and medium resolution: 20 and 15 Å, respectively.

Another sub-group consists of crystals of 50S subunits from 2 thermophilic bacteria, *Bacillus stearothermophilus* [5] and *T thermophilus* [7]. These diffract only to medium resolution (11 Å and 8.7 Å, respectively), but are expected to assist structure determination in a unique fashion. One of these bacteria, (*B stearothermophilus*) could be mutated with thiostrepton to yield ribosomes in which one protein is missing. This mutant was used by us for specific derivatization with super-dense heavy-atom cluster [9]. The crystal form of 50S of *T thermophilus* [7] completes a series consisting of all ribosomal particles (30S, 50S and 70S) and their complexes with components of protein biosynthesis of the same source. This series should enable the investigation of the conformational changes which take place upon the association of ribosomes from their subunits as well as upon binding of components which participate in protein biosynthesis (*eg* m-RNA, t-RNA, nascent protein chain).

*Correspondence and reprints

To support the X-ray crystallographic analysis, other diffraction methods were employed. These include 3-dimensional image reconstruction from electron micrographs of tilt series of 2-dimensional sheets and neutron crystallography. Results of these studies are described in this paper.

We believe that the prospect of elucidating the molecular structure of the ribosome hinges on the interplay between these methods and their correlation with biochemical, functional, genetic and organometallic studies. This topic is also discussed below.

Electron microscopy as a supporting tool for crystallography

The large size of ribosomal particles, which is an obstacle for crystallographic studies, permits investigation by electron miscroscopy as well as the usage of the electron microscope as a diagnostic tool. We first benefitted from the possibility to follow the initial steps of crystal growth and to detect the tendency for crystallization of native and modified particles. In this manner we obtained results rather rapidly, in contrast to the long time needed for the growth of visible 3-dimensional crystals. In later stages, models reconstructed from the diffraction patterns of tilt sets of 2-dimensional sheets are being used for tentative phasing of the crystallographic data at low resolution.

Several limitations are common to image reconstruction and visualization of single particles by electron microscopy. These arise from the difficulties of preserving biological specimens in the microscope vacuum, from uncontrolled shrinkage, from radiation damage, from the influence of the staining procedure on the resulting model and from the uncertainties in choosing the contouring level which defines the envelope of the investigated particle.

However, there are fundamental differences between structure analyses of isolated particles and of 2-dimensional ordered sheets. Whereas visualization of isolated particles is rather subjective, the reconstruction from crystalline materials (such as ordered 2-dimensional sheets) is based on diffraction data and thus is inherently of a more objective character. In addition, isolated particles tend to lie on the grids used for electron microscopy in a few preferred orientations. As a result of the contacts of the particles with the flat grids, their projected views are likely to be distorted. In contrast, particles within the crystalline sheets are held together by interparticle contacts. These contacts construct a network which stabilizes the conformation of the particles and decreases, or even eliminates, the influence of the flat surfaces of the grids.

The advantages of 3-dimensional image reconstruction from tilt series of ordered 2-dimensional sheets of ribosomal particles can be demonstrated in the cases of whole ribosomes from chick embryo [10] and *B stearothermophilus* [11] as well as of 50S ribosomal subunits from the latter [12]. For both, the reconstructed models show key features which could not be detected otherwise. Unfortunately, even the models obtained by image reconstruction from 2-dimensional sheets suffer from several uncertainties, the reasons for which are inherent in the method. These are addressed in some detail below.

Another information source are positively stained embedded thin sections of 3-dimensional crystals. Investigated by electron-microscopy, these sections may facilitate the location of the particles within the crystals even in the early stages of growth. Furthermore, in preferred situations, they can be used for 3-dimensional image reconstruction at low resolution. However, whereas 2-dimensional sheets can be stained negatively and/or positively, thin sections of embedded crystals must be positively stained. Therefore, when reconstructed, they may yield information about the distribution of selected internal components which interact with the positive stain (*eg* rRNA with uranyl acetate). The interpretation of the images is hampered by uncertainty as to the factors governing the stain distribution within the particle, with a somewhat undefined chemical nature.

Three-dimensional image-reconstruction studies on positively stained thin sections of 3-dimensional crystals of large ribosomal subunits from *B stearothermophilus* indicate that most of the ribosomal RNA is located in 2 domains in the core of the particle [13], whereas the proteins are located closer to the surface. This is in agreement with results obtained from unstained 2-dimensional sheets of ribosomes from chicken and lizard, which show that rRNA-rich regions are concentrated in the interior of the ribosomes as well as in the interface area between the large and small subunits [10].

Assessment of the reliability of the reconstructed models

Approximate models of the 70S ribosome and its 50S subunit from *B stearothermophilus* were reconstructed at low resolution, namely 47 Å [11] and 28 Å respectively [12]. Despite their low resolution, the comparison of the various reconstructed images provided a tool for initial assessment of the reliability of these models as well as for a tentative assignment of several functional features [1, 2, 14].

We examined the degree of fit between models obtained by different reconstructions. We compared the shapes of a few images of 70S ribosome and of the 50S subunit as well as the reconstructed images for the latter at 2 different resolution limits (fig 1). Despite the variations in details of the different re-

constructions, there are significant similarities in overall shapes and in the specific features of these particles.

We also compared the shapes of the whole ribosome with its large subunit [1, 14]. The part of the ribosome which was associated with the 50S subunit was found to be rather similar to the unbound particle (fig 1c). The differences, observed mainly in 2 regions, may reflect conformational changes occurring upon association of the subunits, or are a consequence of the low resolution of the reconstructions.

As mentioned above, reconstructed models suffer from several uncertainties which are inherent in the method. A major part of these uncertainties is due to the unknown amount of the shrinkage in the electron microscope vacuum and to the subjectivity in the choice of the level of contouring. It is noteworthy that for negatively stained sheets the resulting models are being defined as regions of stain-rejection.

Another source of uncertainty is due to the fact that the reconstructions are performed using diffraction data of 2-dimensional sheets. Being monolayers, their periodic order is expressed only in 2-dimensions. Thus, the structural elements along the length and the width of these sheets can be directly determined, whereas the depth of the monolayer (the so-called c axis) has to be interpolated. Placed on electron microscopy grids, they can be viewed only in projection, and the contribution of the third dimension to the diffraction pattern is estimated from tilt-sets of the electron-microscopy grids. The limitation in the tilt angle leads to large 'missing cones' in the diffraction data-sets in the direction perpendicular to the plane of the sheet. These in turn cause deformation of the reconstructed images. Hence, it is generally assumed that the determination of the depth as well as the structural elements along the c axis may bear a mistake of up to a third of the thickness of the reconstructed model.

To partially account for the shrinkage, we compared the dimensions of the unit cell of the 2-dimensional sheets of the 70S ribosome with the corresponding vectors in the cell of the 50S subunits. A reasonable fit between these 2 was obtained when the 70S particle was expanded by 10% along the a axis, and that of the 50S particle by 8% along the b axis of each respective unit cell [14]. In this manner we could account for the relative non-isotropic shrinkage of the sheets of the 50S subunits and the 70S ribosomes.

The extent of these expansions is lower than commonly observed in electron microscopy. Hence, we assumed that these corrections do not take account of the entire shrinkage of the ribosomal particles within their 2-dimensional sheets. More objective and complete assessment became possible when data from X-ray and neutron crystallographic experiments became available. These studies are described below.

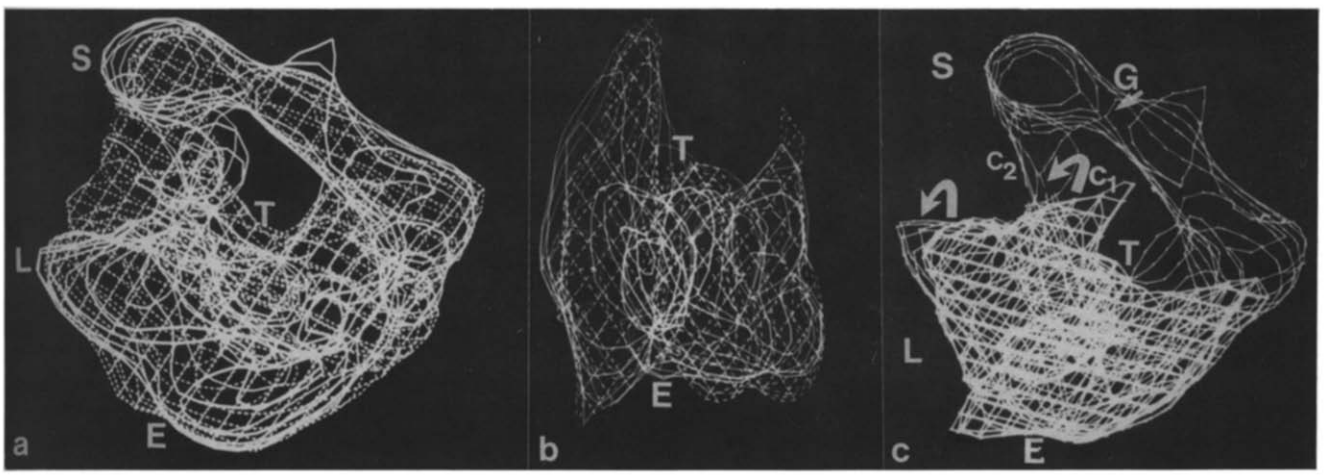

Fig 1. Superposition of 2 independent reconstructions of (a), the 70S ribosome at 50 Å; and (b), 2 50S particles reconstructed at 30 Å resolution. (c), The outline of the reconstructed models of the 70S ribosome (in lines) and of the 50S ribosomal subunit (as a net). (S) and (L) indicate the small (30S) and the large (50S) subunits, respectively. (G) marks the groove rich in RNA in the small subunit. (T) shows the cleft and the entrance to the tunnel and (E) shows the exit site. (C1) and (C2) indicate regions of extra density in the models of the 50S subunit and the 70S ribosome, respectively. The curved arrows indicate possible directions for a cooperative movement at these regions.

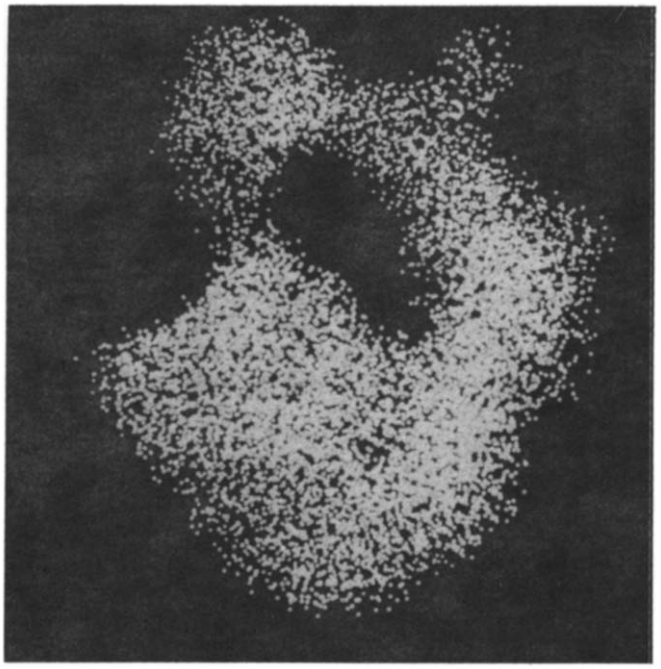

Fig 2. The 70S ribosome represented by 3 000 group scatterers, each accounts for approximately 45 non-hydrogen atoms.

Approaches for phasing at low resolution

Electron density maps, the basis for the determination of 3-dimensional structures, are constructed by Fourier summation of all the reflections which appear in the diffraction pattern of any crystalline compound. Each reflection is a wave characterized by its direction, amplitude and phase. The directions and amplitudes can be measured, whereas phases cannot be directly determined.

For the determination of the low resolution phases we are exploiting the reconstructed models in 2 ways. They serve as starting objects for rotation and translation searches, using the X-ray crystallographic data, as well as for pattern-analysis of the density maps derived from X-ray and neutron diffraction data.

In this study we report preliminary results obtained by using the reconstructed models of the 70S ribosomes and the 50S subunits of *B stearothermophilus* for systematic searches for the most probable packing arrangements in 3-dimensional crystals of 70S ribosomes from *T thermophilus* [8] and 50S subunits of *H marismortui* [3]. The usage of the reconstructed images of ribosomal particles of one bacterial source together with the data obtained from crystals of ribosomal particles from 2 other sources was based on the assumption that the gross structures of ribosomes from different sources are rather similar at medium resolution.

The 70S ribosome

Attempts for packing the reconstructed model of the 70S ribosomes in its crystallographic unit cell showed that a further increase of the volume of the models produced reasonable interparticle nets. Thus, we have expanded the plana dimensions of the image of the 70S particle (plane of fig 2) by 18–20%, and the third dimension by ≈ 30%. These larger particles are, within the experimental errors, of dimensions similar to those determined by other physical methods [15, 16].

The expanded envelope of the 70S ribosome was used for the construction of a pseudo-macromolecule containing a large number of 'group scatterers'. These scatterers were initially positioned on the grid points of the portion of the reconstructed density map, which was assigned to the ribosome. To avoid non-realistic inernal regularities the positions of these scatterers were randomized. Each one was moved within a rectangular box of dimensions equal to the inter-grid distances. The magnitude and the direction of the displacement were determined using a uniform distribution random number generator [17]. The resulting model contained 8 900 scatterers, each representing about 15 non-hydrogen atoms.

The pseudo-macromolecule was employed in real- and reciprocal-space molecular replacement procedures using the packages ULTIMA [18], MERLOT [19], and X-PLOR [20] together with the low resolution (50 Å) X-ray crystallographic data. These efforts yielded several distinct packing arrangements with R factors of around 40–53%. To improve the starting phases, these arrangements are currently being subjected to rigid-body refinement and solvent flattening procedures.

The 50S subunit

Low resolution crystallographic data

A similar approach was employed for investigating the packing modes of the 50S subunits from *H marismortui*. Although these crystals diffract X-rays to relatively high resolution, 3.2 Å [3], we began our search with very low resolution terms, initially up to 50 Å and then to 24 Å.

Neutron diffraction studies

Single crystal neutron diffraction is a technique which facilitates the elucidation of selective structural elements by contrast variation. It is based on the fact that the interactions of neutrons with atoms do not depend on their atomic numbers. Thus, atoms with

similar atomic numbers may diffract neutrons according to very different scattering cross-sections. An appropriate example is the hydrogen whose diffracting power is radically different from that of deuterium.

Since ribosomes are composed of 2 distinctly different chemical entities, proteins and RNA, it is possible to match the contrast (*ie* the diffracting power) of either of them with that of the solvent within the crystals by changing the relative concentrations of D_2O and H_2O [21]. Diffraction is measured at a series of contrasts, and information about the internal distribution of the different components can be obtained. Apart from its intrinsic interest, in principle this information can be used for the determination of the phases [22–24].

The main factor which determines the feasibility of neutron crystallography is the average intensity of the reflections. In general the signals obtained by the diffraction of neutrons are rather weak and necessitate long measuring periods. Here we report our initial attempts in this field.

Neutron diffraction data were collected up to 30 Å resolution from crystals of 50S ribosomal subunits from *H marismortui*. Recently developed *ab initio* methods were employed for phasing these data [25]. Phase sets were generated from normalized structure factors. These sets were selected by a sorting procedure (M Roth and E Pebay-Peyroula, in preparation). The resulting map was relatively clean, and contained several gross features (fig 3). A thorough examination of this map showed that these features are of a shape similar to that obtained by image reconstruction of the same ribosomal subunit from *B stearothermophilus* [12], but with slightly larger dimensions. A proper fit between the map and the reconstructed model of the 50S subunits was obtained when the model was increased by a magnitude similar to that needed for the 70S ribosome. The need for model expansion was substantiated in this case.

The reasonable agreement between the image reconstruction, the X-ray and the neutron diffraction encouraged further investigations. Currently we are engaged in studies which aim to confirm the neutron and X-ray diffraction models by using new phasing techniques. We attempt to apply to these data the *ab intio* phasing method [26] which is based on entropy maximization and maximum likelihood tests. Complementary experiments in a variety of relative D_2O/H_2O should also yield valuable information.

Is the tunnel a universal feature?

The existence of an internal tunnel within the large ribosomal subunit was suggested more than 2 decades ago as a result of several biochemical experiments

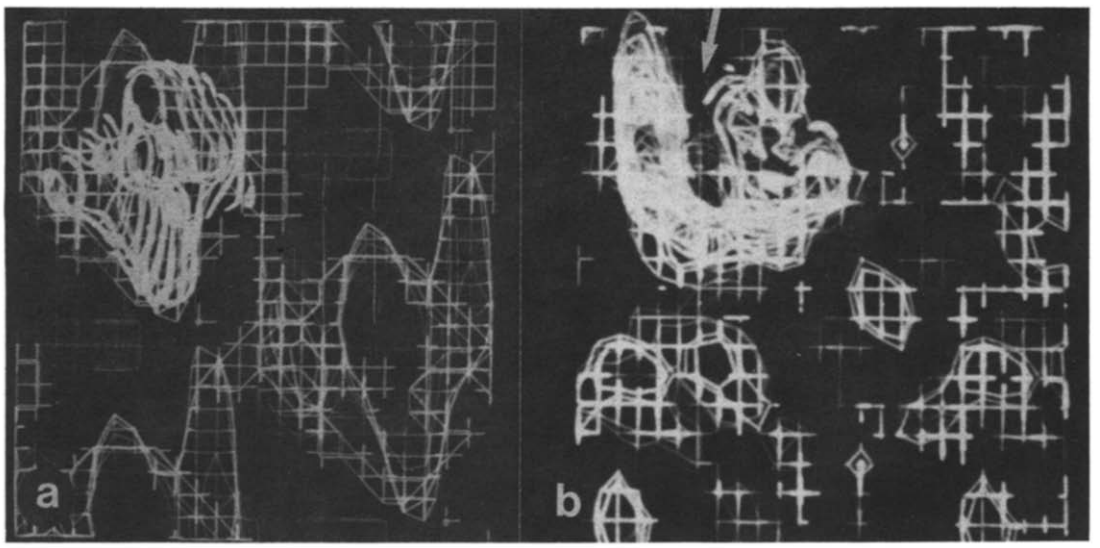

Fig 3. Two views of the density map resulting from the neutron diffraction measurements of crystals of 50S subunits from *H marismortui*, phase by *ab initio* direct methods. 2012 reflections were measured, of which 425 are unique, containing 210 of intensities higher than 3 sigma with an Rsym = 9%. A model of the reconstructed 50S particle of *B stearothermophilus* is superimposed on the map. A single contour map is shown in (a) and a double one in (b). The arrow points to the low density region which could be assigned as the tunnel.

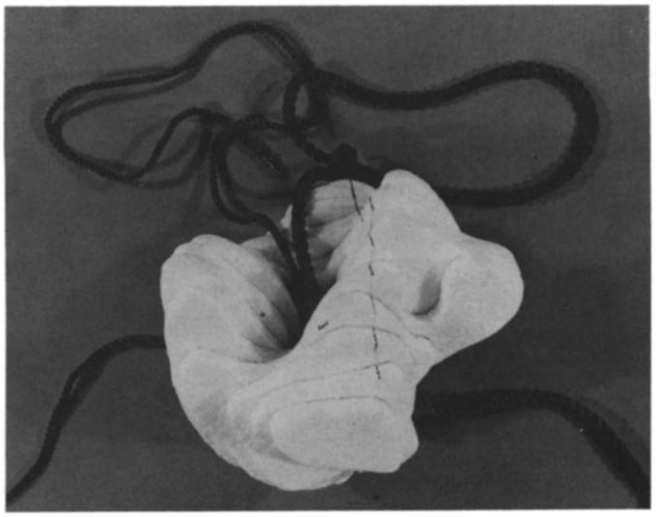

Fig 4. A physical model of the 50S subunit from *B stearothermophilus* as obtained by image reconstruction. The ribbons pass through the main and the side chains [1, 2, 12].

which showed that the ribosome protects the newly synthesized protein chains [27, 28]. More recent biochemical experiments confirm this suggestion [29–36].

Due to experimental constraints, the tunnel could be revealed only recently. It was first observed in reconstructed images of 80S ribosomes packed in 2-dimensional arrays, as a narrow elongated region of low density. This region originates at the subunit's interface and passes through the large ribosomal subunit to a point close to the membrane attachment site [10]. By using the same method, image-reconstruction, we could detect a similar tunnel in 70S ribosomes and 50S ribosomal subunits from *B stearothermophilus* (fig 4) and [11, 12]. Now for the first time, a low density region which resembles the tunnel in dimensions and coincides with its location, was observed in the map obtained from the neutron diffraction data.

These results provide indications for the universality of the inner-ribosomal tunnel. As mentioned above, it has so far been observed in eukaryotic ribosomes as well as in ribosomes of 2 radically different bacteria: *B stearothermophilus*, a mild thermophile, classified as eubacteria, and *H marismortui*, an extreme halophile, classified as archaebacteria.

The possible allocation of the excretion tunnel stimulated a series of experiments aiming at investigating the nature of this path. Recent experiments indicate that ribosomes protect natural proteins more efficiently than artificial homopolypeptides [33] and that, on average, homopolymers choose a path which is different to that of naturally occurring proteins [34].

It is conceivable that the same amino acid appears at the N-terminal of all natural proteins because it possesses a special affinity for the entrance of the tunnel. Using an artificial mRNA which codes for artificial proteins or homopolypeptides which do not start with natural N-terminus, leads to the production of protein chains which lack this affinity. Hence, in the initial stages of the biosynthetic process, a significant part of these polypeptides may not be fixed in space.

Only when the growing chain finds its way into the tunnel does the process of protein biosynthesis continue. This may explain why only 40–60% of any given population of ribosomes are active in protein biosynthesis, whereas almost all of them bind tRNA [37] and why there is a marked difference between the behavior of short and long segments of newly synthesized polylysine or polyphenylalanine [34].

Genetic, biochemical and metallo-organic methods employed for quantitative and specific labeling of ribosomes

The most common method for phasing the diffraction data of macromolecules is that of multiple isomorphous replacement (MIR). This method is based on the attachment of heavy atoms to specific sites on the macromolecules. For this aim, due to the large size of the ribosomes, it is essential to use clusters with a core of several heavy metal atoms linked directly to one another. Such clusters comprise systems of particularly high electron density [38].

To obtain specific binding, we have designed a monofunctional reagent of an undecagold cluster (M_r = 6200). This was covalently and quantitatively bound to free specific sulfhydryl groups on the surface of the ribosome or to isolated ribosomal components which were subsequently incorporated into depleted ribosomal cores [9].

Mutation with thiostrepton led to the growth of *B stearothermophilus* with ribosomes lacking one ribosomal protein BL11. The monofunctional undecagold cluster was bound quantitatively to the isolated protein, and the modified protein was subsequently incorporated into the mutated core to form labelled 50S subunits. The cluster-labelled 50S subunits were crystallized in 2-dimensional sheets and in 3-dimensional crystals, isomorphous with the native ones [9].

Crystallographic data have been collected from crystals of native particles, from the mutated and from the gold-derivatized subunits. The resulting difference Patterson maps contain features which can be associated with the heavy atom cluster.

These studies show that it is possible to label ribosomes by specific covalent binding of heavy-atom clusters without introducing major changes in their

crystallizability, integrity, conformation and biological activity. Hence, the attachment of heavy-metal clusters to isolated ribosomal components, followed by reconstitution of the modified compound into the core particles, provides a useful tool for phase determination.

Extending these procedures to ribosomes from *H marismortui* and *T thermophilus* met with considerable difficulties. However, in a related experiment it was shown that protein L12 from *Methanococal vanniellii* was detached and incorporated into cores of ribosomes of *H marismortui* missing the homologous protein [39].

The tentative assignments on the reconstructed models influenced the design of crystallizable complexes, mimicking ribosomes at defined functional states

A natural consequence of the assignment of the ribosomal features was the crystallization of biologically meaningful complexes. We first crystallized 50S subunits with a tRNA molecule and a short polypeptide fragment [1, 5, 36]. Although not yet ripe for crystallographic studies, the very fact that we could co-crystallize ribosomal particles with short segments of the nascent chain opens new possibilities for the design of interesting systems.

Later on we designed and crystallized complexes of whole 70S ribosomes, mimicking protein biosynthesis. We assumed that the intersubunit free space contributes to the internal flexibility of the ribosome, manifesting itself by allowing for the dynamics involved in the process of biosynthesis of proteins, as well as in the poor resolution of the crystals of 70S ribosomes. Thus, based on our tentative functional assignments (fig 5), we have designed a series of complexes, each of which mimics a stage in protein biosynthesis and contains ribosomes in which the motional freedom is limited. For preliminary assessment of the suitability of such complexes we selected one composed of ribosomes together with a chain of 35 uridines (as mRNA) and 2 molecules of phe-tRNA-(phe). The crystals of this complex grow readily and diffract to 15 Å, compared to those of isolated 70S ribosomes which grow with difficulty and diffract only to 20–24 Å [6, 40].

High resolution data obtained from isolated ribosomal components should aid phasing

Despite extensive efforts, so far only a few isolated ribosomal components could be crystallized, and only a few of them were subjected to crystallographic analysis which matured in a detailed molecular structure. This may indicate that the intraparticle interactions contribute significantly to the stabilization of the conformation of the whole assembled ribosome. Furthermore, it may show that many ribosomal components lose their *in situ* conformation when they are detached from their supporting environment.

Hence, we attempted to purify *in situ* complexes of ribosomal components with a defined composition, high stability and relatively low molecular weights. Assuming that they maintain their natural conformation, we hope that they will yield well-ordered crystals. The isolation of such a complex from *H marismortui* (HL8 with 23S RNA) is in progress.

Conclusions

Structural studies provide static information, but at the same time may lead to the design of subsequent functional and dynamic experiments. We have shown that merging results from X-ray and neutron crystallography, electron microscopy and image reconstruction

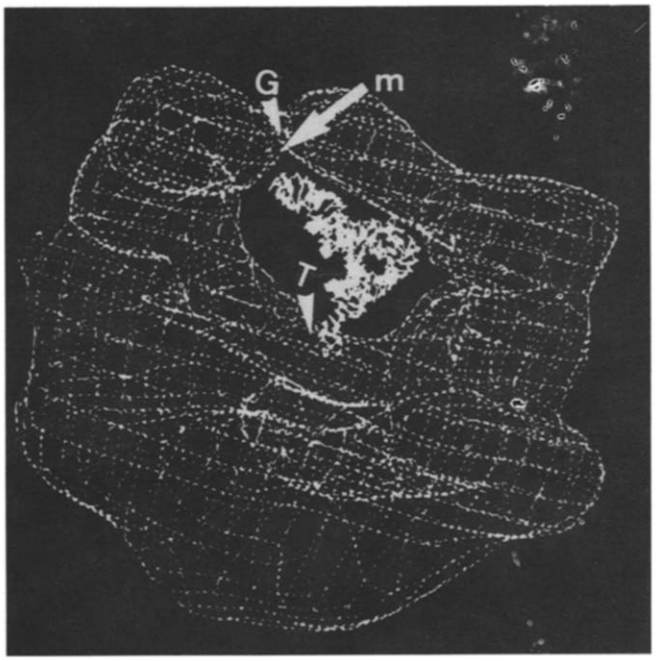

Fig 5. The reconstructed model of the 70S ribosome into which a molecule of tRNA was 'model-built', so that its anticodon loop is in the proximity of the mRNA (M) which passes through the groove (G) in the 30S subunit and the CCA end points toward the entrance of the tunnel T [1, 14].

together with information concerning the function as well as the genetic, chemical and physical properties of ribosomes, enabled the construction of sophisticated tools for overcoming some of the limitations of traditional structural approaches.

Acknowledgments

All stages of the studies presented here were carried out in active collaboration and under the inspiration and the guidance of the late Prof HG Wittmann. We would like to thank D Rabinovitch, A Bentely-Lewitt, P Metcalf, N Volkmann, P Rehse, WS Bennett, HAS Hansen, K vonBöhlen, K Leonard, W Jahn, U Evers, H Bertels, H Hope, F Frolow, C Kratky and A Zaitzev-Bashan for their active participation in some aspects of this work, J Müssig, I Makowski, J Piefke, C Glotz, T Arad, J Halfon, B Romberg, R Hansenbank, S Hottenträger, P Webster, C Paulke, B Dressler, S Meyer, M Laschever, Y BenIsrael, B Donzelmann, G Idan and A Bruhnsen for their skillful technical assistance. This work was carried out at the Max-Planck Institute for Molecular Genetics in Berlin, the Weizmann Institute of Science, the Max-Planck Research Unit at DESY/Hamburg, the ILL neutron-diffraction facility in Grenoble, EMBL Laboratory in Heidelberg and at the following synchrotron facilities: EMBL/DESY Hamburg, CHESS/Cornell Univ, SSRL/Stanford Univ, SRS/Daresbury/UK and KEK/Japan. The study was supported by BMFT (05 180 MP BO), NIH (GM 34360), BSF (85-00381), Heinemann (4694 81), NCRD (France-Israel Binational Foundation) (334190) and Minerva research grants. AY holds the Martin S Kimmel Professorial chair.

References

1 Yonath A, Wittmann HG (1989) *Trends Biochem Sci* 14, 329–333
2 Yonath A, Bennett WS, Weinstein S, Wittmann HG (1990) *In: The Ribosome: Structure, Function and Evolution* (Hill W, ed) ASM Publications, 134–147
3 Makowski I, Frolow F, Saper MA, Wittmann HG, Yonath A (1987) *J Mol Biol* 193, 819–821
4 Yonath A, Glotz C, Gewitz HS, Bartels KS, von Böhlen K, Markowski I, Wittmann HG (1988) *J Mol Biol* 203, 831–834
5 Müssig J, Makowski I, von Böhlen K, Hansen HAS, Bartels KS, Wittmann HG, Yonath A (1989) *J Mol Biol* 205, 619–621
6 Hansen HAS, Volkmann N, Piefke J, Glotz C, Weinstein S, Makowski I, Meyer S, Wittmann HG, Yonath A (1990) *Biochim Biophys Acta* 1050, 1–7
7 Volkmann N, Hottenträger S, Hansen HAS, Zaytsev-Bashan A, Sharon R, Berkovitch-Yellin Z, Yonath A, Wittmann HG (1990) *J Mol Biol* 216, 239–241
8 Berkovitch-Yellin Z, Hansen HAS, Bennett WS, Sharon R, von Böhlen K, Volkmann N, Piefke J, Yonath A, Wittmann HG (1990) *J Crystal Growth* 110, 208–211
9 Weinstein S, Jahn W, Wittmann HG, Yonath A (1989) *J Biol Chem* 264, 19138–19142
10 Milligan RA, Unwin PNT (1986) *Nature (Lond)* 319, 693–696
11 Arad T, Piefke J, Weinstein S, Gewitz HS, Yonath A, Wittmann HG (1987) *Biochimie* 69, 1001–1005
12 Yonath A, Leonard KR, Wittmann HG (1987) *Science* 236, 813–816
13 Leonard KR, Arad T, Tesche B, Erdmann VA, Wittmann HG, Yonath A, (1982) *In: Electron Microscopy 1982*. Offizin Paul Hartung, Hamburg, vol 3, 9–30
14 Berkovitch-Yellin Z, Wittmann HG, Yonath A (1990) *Acta Crystallogr* B46, 637–643
15 Wittmann HG (1983) *Annu Rev Biochem* 52, 35–65
16 Hardesty B, Kramer G (1986) *In: Structure, Function and Genetics of Ribosomes*. Springer Verlag, Heidelberg, New York
17 *NAG Fortran Library Manual*, Mark 11, vol 5
18 Rabinovich D, Shakked Z (1984) *Acta Crystallogr* A40, 195–199
19 Fitzgerald PM (1988) *J Appl Crystallogr* 21, 273–279
20 Brunger AT (1988) *X-PLOR Manual, Version 1.5*. Yale Univ, New Haven, CN, USA
21 Jacrot B (1976) *Rep Prog Phys* 39, 911–953
22 Roth M, Lewit-Bentley A, Michel H, Deisenhofer J, Huber R, Oesterheld D (1989) *Nature (Lond)* 340, 659–663
23 Podjarny A, Rees B, Thierry JC, Cavarelli J, Jesior JC, Roth M, Lewit-Bentley A, Kahn R, Lorber B, Ebel JP, Giege R, Moras D (1987) *J Biomol Struct & Dyn* 5, 187–191
24 Bentley GA, Lewit-Bentley A, Liljas L, Skoglund U, Roth M, Unge T (1987) *J Mol Biol* 194, 129–135
25 Roth M (1990) Bischenberg summer school, Aug 1990
26 Bricogne G, Gilmore CJ (1990) *Acta Crystallogr* A46, 284–297
27 Malkin LI, Rich A (1967) *J Mol Biol* 26, 329–346
28 Blobel G, Sabatini DD (1970) *J Cell Biol* 45, 130–145
29 Smith WP, Tai PC, Davis BD (1978) *Proc Natl Acad Sci USA* 75, 5922–5925
30 Yen IJ, Macklin PS, Cleavland DW (1988) *Nature (Lond)* 334, 580–585
31 Ryabova LA, Selivanova OM, Baranov VI, Vasiliev VD, Spirin AS (1988) *FEBS Lett* 226, 255–260
32 Evers U, Gewitz HS (1989) *Biochem Int* 19, 1031–1034
33 Kolb VA, Kommer A, Spirin AS (1990) *Workshop on Translation*. Leiden, 84a
34 Hardesty B, Picking WD, Odom OW (1990) *Biochim Biophys Acta* 1050, 197–202
35 Kurzchalia SV, Wiedmann M, Breter H, Zimmermann W, Bauschke E, Rapoport TA (1988) *Eur J Biochem* 172, 663–668
36 Gewitz HS, Glotz C, Piefke J, Yonath A, Wittmann HG (1988) *Biochimie* 70, 645–648
37 Rheinberger HJ, Nierhaus KH (1990) *Eur J Biochem* 193, 643–650
38 Jahn W (1989) *Z Naturforsch* 44b, 79–82
39 Köpke AKE, Paulke C, Gewitz HS (1990) *J Biol Chem* 265, 6436–6440
40 Trakhanov SD, Yusupov MM, Shirokov VA, Garber MB, Mitschler A, Ruff M, Thierry JC, Moras D (1989) *J Mol Biol* 209, 327–328